

Modeling, Simulation, Inversion and Chang-E 1 Data Validation for Passive/Active Microwave Remote Sensing of Lunar Surface Media

Ya-Qiu Jin and Wenzhe Fa

Key Laboratory of Wave Scattering and Remote Sensing Information (MoE)

Fudan University, Shanghai 200433, China

Email: yqjin@fudan.edu.cn

Abstract

In China's first lunar exploration project, Chang-E 1 (CE-1), a multi-channel (3.0, 7.8, 19.35 and 37GHz) microwave radiometer in passive microwave remote sensing, was first aboard the satellite, with the purpose of measuring microwave brightness temperature from lunar surface and surveying the global distribution of lunar regolith layer thickness.

In this paper, the three-layer model of lunar surface media, i.e. top soil layer, regolith layer and underlying rock media as shown in Fig. 1, is presented.

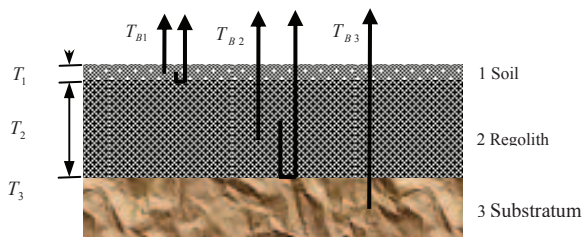


Fig. 1 Three-layer emission model of lunar surface media.

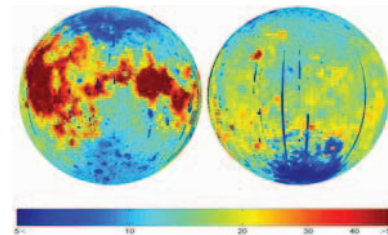


Fig. 2 Evaluation of global ^3He in regolith media

A correspondence of the lunar regolith layer thickness to the lunar digital elevation mapping is proposed to tentatively construct the global distribution of lunar regolith layer thickness. Using Clementine UVVIS multispectral data, the global spatial distribution of $\text{FeO}+\text{TiO}_2$ content on the lunar regolith layer is calculated. The dielectric permittivity of global lunar regolith media are obtained based on the relationship between dielectric permittivity, bulk density and $\text{FeO}+\text{TiO}_2$ content. Based on some measurements of physical temperature of the lunar surface, an empirical formula of physical temperature distribution over the lunar surface is presented. Using fluctuation dissipation theorem and radiative transfer of stratified media, numerical simulations of multi-channel brightness temperature (T_b) from global lunar surface are obtained. It is applied to analyze and retrieve the regolith layer thickness, and finally to evaluate global distribution of ^3He content in regolith media derived from global distribution of solar flux and lunar surface optical maturity.

The primary 621 tracks of swath data measured by CE-1 microwave radiometer from November 2007 to February 2008 are collected and analyzed.

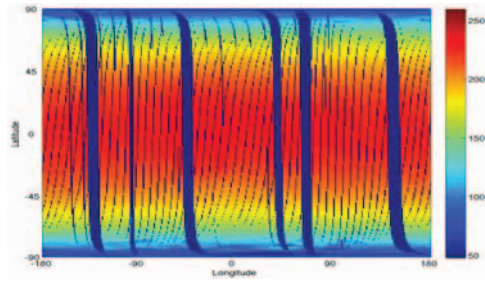


Fig. 3 Tb data observed by CE-1 radiometer at 3.0GHz.

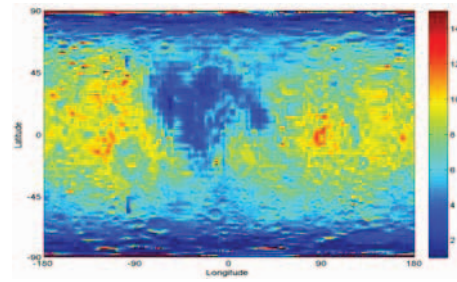


Fig. 4 Inverted regolith thickness from CE-1 Tb.

Using nearest neighbor interpolation based on the sun incidence angle in observations, global distributions of Tb from lunar surface at lunar daytime and nighttime are constructed. Using the three-layer model for microwave thermal emission of lunar surface, the Tb measurements and its dependence upon latitude, frequency and $\text{FeO}+\text{TiO}_2$ content, etc. are discussed. On the basis of the ground measurements at Apollo landing sites, the observed Tb at these locations are validated and calibrated by numerical three-layer modeling. Lunar surface temperature is first determined by high frequency channels Tb, such as 19 and 37GHz. Using the empirical dependence of physical temperature upon the latitude verified by the measurements at Apollo landing sites, the global distribution of regolith layer thickness is then inverted from the Tb data of CE-1 at low 3GHz channel. Those inversions at Apollo landing sites are compared with the Apollo *in situ* measurements. Finally, the statistical property of regolith thickness distribution is analyzed and discussed.

In active microwave remote sensing, based on the statistics of the lunar cratered terrain, e.g. population, dimension and shape of craters, the terrain feature of cratered lunar surface is numerically generated using Monte Carlo (MC) method. According to inhomogeneous distribution of the lunar surface slope, the triangulated irregular network (TIN) is employed to make the digital elevation of lunar surface model. The Kirchhoff approximation of surface scattering is then applied to simulation of lunar surface scattering. The synthetic aperture radar (SAR) image for comprehensive cratered lunar surface is numerically generated using back projection (BP) algorithm of SAR imaging. Making use of the digital elevation and Clementine UVVIS data at Apollo 15 landing site as the ground truth, an SAR image at Apollo 15 landing site is simulated. The image simulation is also verified using real SAR image and echoes statistics.

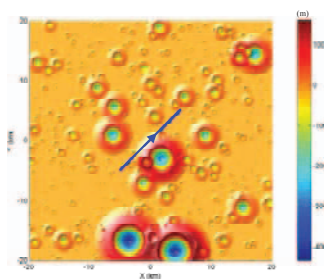


Fig. 5 MC generated Lunar cratered surface.

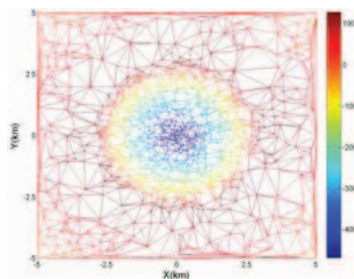


Fig. 6 TIN approach.

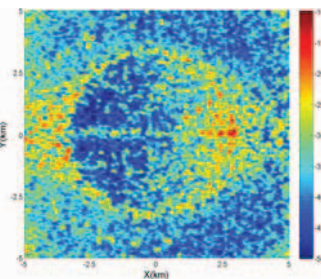


Fig. 7 SAR image of a crater surface.

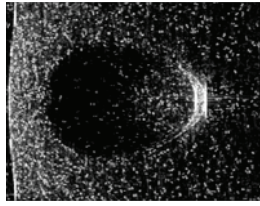


Fig. 8 A simulated SAR image of lunar surface.

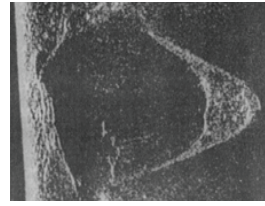


Fig. 9 A real SAR image of lunar surface.

Utilizing the nadir echoes time delay and intensity difference from the surface and subsurface, high frequency (HF) radar sounder is an effective tool for investigation of lunar subsurface structure in lunar exploration. Making use of rough surface scattering and ray tracing of geometric optics, a numerical simulation of radar echoes from lunar layering structures with surface feature, the topography of mare and highland surfaces is developed. Radar echoes and its range images are numerically simulated, and their dependence on the parameters of lunar layering interfaces are described.

Following the lunar surface feature, the topography of mare and highland surface is generated, and the triangulated irregular network (TIN) is applied to making digital elevation of lunar surface for numerical scattering calculations and range image simulation. Based on Kirchhoff approximation and ray tracing, an effective numerical approach of radar echo simulation from layering structure with rough interfaces is developed. Scattering from the lunar surface and subsurface are numerically calculated. Radar echo image with the radar range is produced, and its dependence upon the surface parameters is discussed.

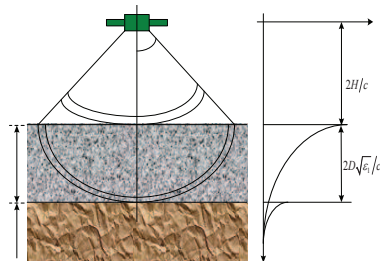


Fig. 10 Principle of HF radar probing of lunar subsurface.

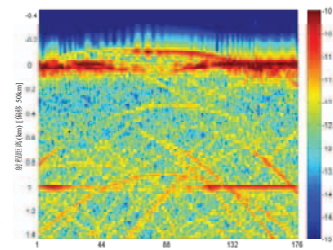


Fig. 11 Radar range echoes image.

References

- [1] W. Fa and Y.Q. Jin, "Simulation of brightness temperature of lunar surface and inversion of the regolith layer thickness", *Journal of Geophysical Research-Planet*, 2007, 112, E05003, doi: 10.1029/2006JE002751: 1-13.
- [2] W. Fa and Y.Q. Jin, "Quantitative estimation of helium-3 spatial distribution in the lunar regolith layer", *ICARUS*, 2007, 71(190): 15-23.
- [3] W. Fa and Y.Q. Jin, "Analysis of Microwave Brightness Temperature of Lunar Surface and Inversion of Regolith Layer Thickness: Primary Results from Chang-E 1 Multi-Channel Radiometer Observation", *ICARUS*, 2010 in press.
- [4] Y.Q. Jin, F. Xu and W. Fa, "Numerical simulation of polarimetric radar pulse echoes from lunar regolith layer with scatter inhomogeneity and rough interfaces", *Radio Science*, 2007, 42, RS3007, doi: 10.1029/RS2006003523: 1-10.
- [5] W. Fa, F. Xu and Y.Q. Jin, "Image simulation of SAR remote sensing over inhomogeneously undulated lunar surface", *Science in China (F)*, 2009, 52(4): 559-574.